Minimum tetragonality in PbTiO3/BaTiO3 ferroelectric superlattices

Liang Hong, Yulan Li, Pingping Wu, and Long-Qing Chen

Citation: Journal of Applied Physics **114**, 144103 (2013); doi: 10.1063/1.4824922
View online: http://dx.doi.org/10.1063/1.4824922
View Table of Contents: http://scitation.aip.org/content/aip/journal/jap/114/14?ver=pdfcov
Published by the AIP Publishing

Minimum tetragonality in $PbTiO_3/BaTiO_3$ ferroelectric superlattices

Liang Hong,[1,a] Yulan Li,[2] Pingping Wu,[1,3] and Long-Qing Chen[1]
[1]*Department of Materials Science and Engineering, The Pennsylvania State University, University Park, Pennsylvania 16802, USA*
[2]*Pacific Northwest National Laboratory, Richland, Washington 99352, USA*
[3]*Department of Physics, University of Science and Technology Beijing, Beijing 100083, China*

(Received 2 September 2013; accepted 24 September 2013; published online 10 October 2013)

$PbTiO_3/BaTiO_3$ ferroelectric superlattices commensurately constrained by a $SrTiO_3$ substrate are studied using both phenomenological theory and phase field simulations. It is found that the spontaneous polarization of the superlattice does not vary significantly with volume fraction until $PbTiO_3$ becomes the majority of the superlattice. A minimum tetragonality exists at room temperature when the $PbTiO_3$ volume fraction is around 90%, resulted from its different sensitivity to epitaxial strains and the electrostatic coupling of the two polarized layers in this $PbTiO_3/BaTiO_3$ superlattice. © *2013 AIP Publishing LLC*. [http://dx.doi.org/10.1063/1.4824922]

Oxide superlattices consist of periodic repetitions of two or more different oxide layers with coherent interfaces between the layers. They may exhibit emergent properties that are not merely volume averages of each constituent layer of oxide. For example, ferroelectric superlattice have been observed to exhibit dramatically enhanced polarizations, permittivity, and switching behavior.[1,2] However, most of the existing studies were focused on superlattices composed of ferroelectric and paraelectric layers, e.g., $BaTiO_3/SrTiO_3$ (BTO/STO)[3–8] and $PbTiO_3/SrTiO_3$ (PTO/STO).[9–13] In such superlattices, the electrostatic and mechanical couplings between the layers may lead to significant induced polarizations or even ferroelectric phase transitions in the paraelectric layers. In this work, we are focused on superlattices with both layers being ferroelectric and study their structures and properties using both phenomenological and phase field approaches.

We consider the specific example of $(PTO)_m/(BTO)_n$ superlattices commensurately grown on a STO substrate. Here, we define a repeated stacking of m unit cells of PTO on n unit cells of BTO as $(PTO)_m/(BTO)_n$. The two ferroelectric layers, PTO and BTO, have different sensitivity to epitaxial strains; PTO has a much larger polar displacement and is less sensitive to the biaxial compressive strains than BTO.[14,15] Our focus is on the effect of polarization-strain and electrostatic couplings in these superlattices on the polarization and tetragonality.

For thermodynamic calculations, the two different layers of the superlattice are treated as individual constrained thin films but coupled through electrostatic and mechanical interactions.[16] As both PTO and BTO layers are under large compressive strains imposed by the STO substrate, the ferroelectric domains with out-of-plane polarizations are more stable than others based on the phase diagrams[17,18] of ferroelectric thin films. The electrostatic couplings between the ferroelectric layers favor uniform our-of-plane polarizations across the different layers to minimize the depolarization field.[16] Thus, the thermodynamic potential of the present ferroelectric superlattice ($\tilde{G}$) can be described by a polynomial in terms of single out-of-plane polarization (P_3). The phase field simulations discussed later validates the present phenomenological model. Then, the thermodynamic potential can be written as

$$\begin{aligned}\tilde{G} &= x\tilde{G}_A + (1-x)\tilde{G}_B \\ &= (x\alpha^*_{3,A} + (1-x)\alpha^*_{3,B})P_3^2 + (x\alpha^*_{33,A} + (1-x)\alpha^*_{33,B})P_3^4 \\ &\quad + (x\alpha_{111,A} + (1-x)\alpha_{111,B})P_3^6 \\ &\quad + (x\alpha_{1111,A} + (1-x)\alpha_{1111,B})P_3^8 \\ &\quad + \left(x\frac{u^2_{m,A}}{s_{11,A}+s_{12,A}} + (1-x)\frac{u^2_{m,B}}{s_{11,B}+s_{12,B}}\right), \end{aligned} \quad (1)$$

where $\tilde{G}_A$ and $\tilde{G}_B$ represent the thermodynamic potentials of PTO and BTO layers, respectively. $x = \frac{m}{m+n}$ is the volume fraction of PTO layers, which is tuned to probe the variations of the ferroelectric properties. The coefficients of different polarization terms and elastic compliances (s_{11} and s_{12}) can be found in Refs. 17, 19, and 20; the renormalized coefficients α^*_3 and α^*_{33} were given in Ref. 17. The in-plane mismatch strains are $u_{m,A} = \frac{(a_A - a_{A0})}{a_{A0}}$, $u_{m,B} = \frac{(a_B - a_{B0})}{a_{B0}}$, $u_{12} = 0$. Here, a_A and a_B are the in-plane lattice parameters of PTO and BTO layers, which are set to be equal to the pseudocubic lattice parameter of substrate STO due to the commensurate constraint, while a_{A0} and a_{B0} are the PTO and BTO pseudocubic lattice parameters, respectively. All the in-plane lattice parameters are listed in Ref. 21, which are obtained from Ref. 22 and 23. The spontaneous polarization can be derived through $\frac{\partial \tilde{G}}{\partial P_3} = 0$. Then, we can get the tetragonality $\frac{c}{a} = x\frac{1+S_{3,A}}{1+u_{m,A}} + (1-x)\frac{1+S_{3,B}}{1+u_{m,B}}$, where strain $S_3 = \frac{2s_{12}}{s_{11}+s_{12}}u_m + (Q_{11} - \frac{2s_{12}Q_{12}}{s_{11}+s_{12}})P_3^2$. Q_{11} and Q_{12} are electrostrictive constants.

At small volume fraction of PTO, the polarization increases slightly with volume fraction, while at very high volume fraction, it increases rapidly as shown in Figure 1(a).

[a]Author to whom correspondence should be addressed. Electronic mail: lxh42@psu.edu.

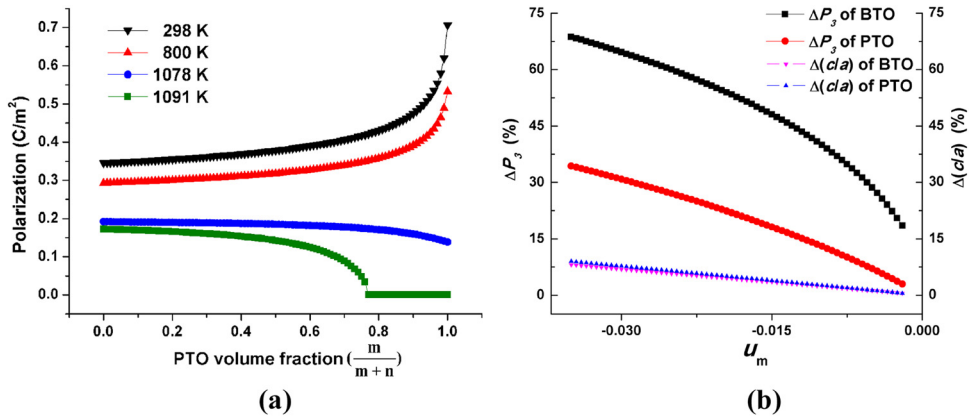

FIG. 1. Thermodynamic calculations of polarization variation with PTO volume fraction $\left(\frac{m}{m+n}\right)$ in $(PTO)_m/(BTO)_n$ superlattices under different temperatures (a), and the polarization and tetragonality enhancement as a function of mismatch strain u_m in individual BTO and PTO films (b).

Figure 1(b) gives the comparisons of polarization and tetragonality enhancement of BTO and PTO films at room temperature under the mismatch strain $u_m = -0.2\% \sim -3.5\%$ (bracketing the misfit strain values of $u_{m,A} = -0.76\%$, $u_{m,B} = -2.39\%$ for the individual layers), within which only c-domains are stable in both films.[17,18] We define $\Delta P_3 = \frac{[P_3(u_m) - P_3(0)]}{P_3(0)}$, where $P_3(0)$ is the thin film polarization along the thickness direction with zero mismatch strain; $\Delta(c/a)$ is defined in the same way. It is clearly seen from Figure 1(b) that the polarization of BTO film increases faster than that of PTO film under the same compressive strain. In other words, the polarization of BTO films is more sensitive to the epitaxial mismatch strain than that of PTO films although they have similar tetragonality enhancement and agree with prior first-principles[14] and thermodynamic[15] calculations.

Cooper and Rabe[24] argued that the stiffer BTO energy potential determines the slow increase of saturated polarization in the BTO layers. It should be noticed that the strain effect on BTO is more significant than on PTO due to the much larger lattice parameter difference between BTO and STO substrate than between PTO and STO. As a result, at high temperatures where PTO layers become paraelectric and BTO layers remain to be ferroelectric with smaller spontaneous polarization, a sluggish variation in polarization with PTO volume fraction is observed (Figure 1(a)). This is quite different from the behavior of ferroelectric/paraelectric (FE/PA) superlattices, e.g., PTO/STO, in which the polarization in PTO layers is sensitive to its volume fraction change.[25] Thus, due to the stronger impact of epitaxial strain on BTO than PTO (Figure 1(b)), the polarization in BTO layers does not vary significantly with PTO volume fraction until PTO layers become the majority phase in the superlattice.

There exists a critical volume fraction at which the polarization in the FE/PA superlattice disappears. This critical volume fraction can be obtained with the same approach as described in Ref. 16, by neglecting the sixth-order and eighth-order terms of P_3. The transition temperatures of PTO and BTO films on STO substrates are 1085 K and 1106 K, respectively (Figure 2(b)). Thus at 1091 K PTO/BTO is a FE/PA superlattice, and the critical volume fraction[16] is $x \approx \frac{\alpha^*_{3,B}}{-\alpha^*_{3,A} + \alpha^*_{3,B}} = 0.77$, which agrees well with Figure 1(a).

Figure 2(a) presents the tetragonality of the ferroelectric tetragonal phase of PTO/BTO superlattice versus PTO volume fraction. It is seen that a minimum tetragonality always exists in the PTO/BTO superlattices below a critical temperature. The minimum point can be obtained through substituting S_3 into tetragonality expression; then we get

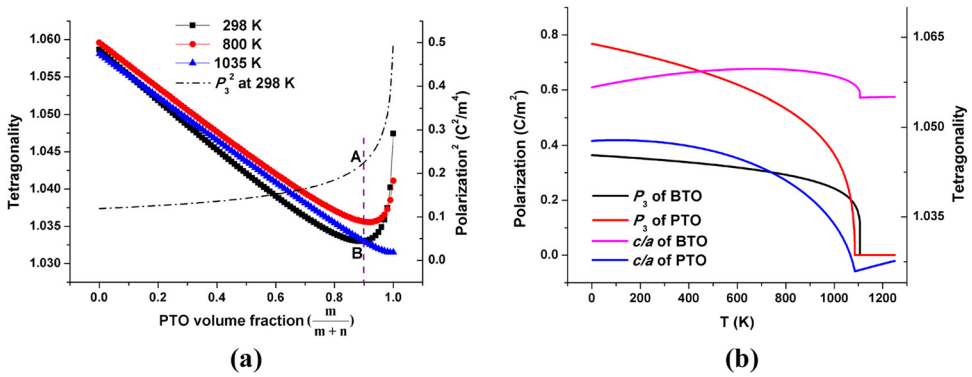

FIG. 2. Tetragonality variation with PTO volume fraction $\left(\frac{m}{m+n}\right)$ at different temperatures (a). The dashed-dotted black line describes the variation of P_3^2, and the dash purple line represents the volume value at which the tetragonality reaches minimum at room temperature. A and B are the points at which purple line crosses the P_3^2 and tetragonality variation lines at room temperature, respectively. (b) Plots of polarization and tetragonality versus temperature for individual BTO and PTO films on STO substrates.

$$\frac{c}{a} \approx \frac{1+\dfrac{2s_{12,B}}{s_{11,B}+s_{12,B}}u_{m,B}+\left(Q_{11,B}-\dfrac{2s_{12,B}Q_{12,B}}{s_{11,B}+s_{12,B}}\right)P_3^2}{1+u_{m,B}}+x\left(\frac{1+\dfrac{2s_{12,A}}{s_{11,A}+s_{12,A}}u_{m,A}}{1+u_{m,A}}-\frac{1+\dfrac{2s_{12,A}}{s_{11,A}+s_{12,A}}u_{m,A}}{1+u_{m,B}}\right). \quad (2)$$

The minimum tetragonality is reached as $\frac{\partial(c/a)}{\partial x}=0$, thus

$$\frac{\partial(P_3^2)}{\partial x}=-\left(\frac{1+\dfrac{2s_{12,A}}{s_{11,A}+s_{12,A}}u_{m,A}}{1+u_{m,A}}-\frac{1+\dfrac{2s_{12,A}}{s_{11,A}+s_{12,A}}u_{m,A}}{1+u_{m,B}}\right)\Bigg/\left(\frac{Q_{11,B}-\dfrac{2s_{12,B}Q_{12,B}}{s_{11,B}+s_{12,B}}}{1+u_{m,B}}\right). \quad (3)$$

At room temperature, we get the minimum tetragonality 1.033 when PTO volume is 0.9 and $\frac{\partial(P_3^2)}{\partial x}$ equals 0.56, which agrees well with the results in Figure 2(a) and from first-principle calculations.[24] With the increase of temperature, the PTO volume at which superlattice tetragonality approaches the minimum increases. Above 1038 K, the superlattice tetragonality decreases linearly with the increase of PTO volume, and there is no minimum point. Below the transition temperature, tetragonality of individual BTO films shows a weak dependence on temperature due to the large epitaxial strain induced by the STO substrate (Figure 2(b)). Above the transition temperature, both the tetragonality of PTO and BTO films vary linearly with temperature.

Based on the thermodynamic analysis of the ferroelectric properties of the superlattice assuming a single domain state, we employed the phase field model to simulate the polarization distribution of $(PTO)_m/(BTO)_n$ superlattice on a STO substrate. The simulation cell is discretized as $64\Delta x_1 \times 64\Delta x_2 \times N\Delta x_3$, where $\Delta x_1 = \Delta x_2 = 1$ nm, $\Delta x_3 = 0.5a_{STO} \approx 0.2$ nm, and $N = 2(m+n)$. $x_i = (x_1, x_2, x_3)$ is the superlattice coordinate. Periodical boundary conditions are employed along the x_1, x_2, and x_3 directions. The strain arising from the substrate constraint is uniform and in plane, and the lattice mismatch between the two layers is part of the stress-free strain. The charges on the top surface and the superlattice/substrate interface are compensated. The free energy coefficients and the elastic and electrostrictive constants also come from Refs. 17, 19, and 20 as in the thermodynamic analysis. More details for constructing the phase field superlattice model as well as all the free energy expressions can be found in Ref. 23.

The simulation starts from an initial paraelectric state with random noise perturbations for the local polarization. Figure 3 displays the stable domain morphology of a $(PTO)_8/(BTO)_9$ superlattice at room temperature where only tetragonal *c*-domains are stable. The simulation size of the present superlattice is 64 nm × 64 nm × 6.8 nm. It is found that the polarization magnitude is almost uniform along the thickness direction of the superlattice, which is different from the BTO/STO superlattices where the polarization magnitude get maximized in the center part of the BTO layers.[23] The polarization distributions arises from the collective polarization-strain and electrostatic dipole-dipole couplings. First of all, both BTO and PTO layers in the superlattice prefer *c*-domains under a large compressive strain. Second, since these two layers are ferroelectric, the electrostatic energy minimization would prefer a uniform polarization magnitude across the superlattice thickness. These observations validate the utilization of single P_3 in the phenomenological description of the present superlattice. The average polarization magnitude and tetragonality of the $(PTO)_8/(BTO)_9$ superlattice are 0.37 C/m^2 and 1.041, respectively, which agree with the results in Figures 1 and 2. We also have carried out other superlattice simulations with different PTO volume fractions through the change of layers thickness while we keep the simulation size unchanged. We observed similar dependence of polarization on PTO volume fraction and also a minimum in the tetragonality at PTO volume fraction of around 90%, i.e., $(PTO)_{15}/(BTO)_2$.

In conclusion, it is found that the polarization of PTO/BTO superlattices is insensitive to the volume fraction of PTO when the volume fraction is below ~90% and then increases rapidly from 90% to 100% as a result of dramatic enhancement of polarization and transition temperature within the BTO layers by the mismatch strain with the STO substrate. This volume fraction dependence of polarization could be exploited in designing compositionally graded ferroelectric thin films to induce large polarization gradient. In addition, both thermodynamic calculations and phase field simulations show the existence of a minimum tetragonality in the PTO/BTO superlattice as a function of PTO volume

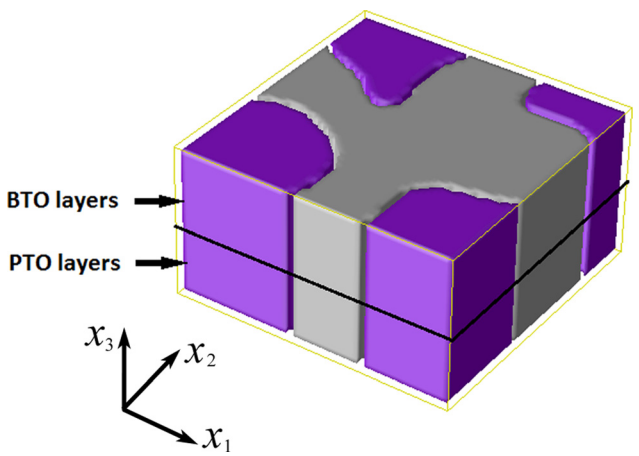

FIG. 3. Domain morphology of a $(PTO)_8/(BTO)_9$ superlattice obtained through a phase field simulation at room temperature. The two colors (purple and grey) in the superlattice represent *c*-domains with up and down polarization dipoles, respectively.

fraction resulted from the combined electrostatic and mechanical interactions within the superlattices.

This work was supported by the NSF through grants DMR-0820404, DMR-1210588, and DMR-1006541. The computer simulations were carried out on the LION and cyberstar clusters at the Pennsylvania State University, in part supported by instrumentation (cyberstar Linux cluster) funded by the NSF through Grant OCI-0821527.

[1]H. N. Lee, H. M. Christen, M. F. Chisholm, C. M. Rouleau, and D. H. Lowndes, Nature **433**, 395 (2005).
[2]P. Zubko, N. Stucki, C. Lichtensteiger, and J. M. Triscone, Phys. Rev. Lett. **104**, 187601 (2010).
[3]H. Tabata, H. Tanaka, and T. Kawai, Appl. Phys. Lett. **65**, 1970 (1994).
[4]J. B. Neaton and K. M. Rabe, Appl. Phys. Lett. **82**, 1586 (2003).
[5]A. Q. Jiang, J. F. Scott, H. B. Lu, and Z. H. Chen, J. Appl. Phys. **93**, 1180 (2003).
[6]W. Tian, J. C. Jiang, X. Q. Pan, J. H. Jaeni, Y. L. Li, L. Q. Chen, D. G. Schlom, J. B. Neaton, K. M. Rabe, and Q. X. Jia, Appl. Phys. Lett. **89**, 092905 (2006).
[7]D. A. Tenne, A. Bruchhausen, N. D. Lanzillotti-Kimura, A. Fainstein, R. S. Katiyar, A. Cantarero, A. Soukiassian, V. Vaithyanathan, J. H. Haeni, W. Tian, D. G. Schlom, K. J. Choi, D. M. Kim, C. B. Eom, H. P. Sun, X. Q. Pan, Y. L. Li, L. Q. Chen, Q. X. Jia, S. M. Nakhmanson, K. M. Rabe, and X. X. Xi, Science **313**, 1614 (2006).
[8]K. Kathan-Galipeau, P. P. Wu, Y. L. Li, L. Q. Chen, A. Soukiassian, X. X. Xi, D. G. Schlom, and D. A. Bonnell, ACS Nano **5**, 640 (2011).
[9]J. C. Jiang, X. Q. Pan, W. Tian, C. D. Theis, and D. G. Schlom, Appl. Phys. Lett. **74**, 2851 (1999).
[10]M. Dawber, C. Lichtensteiger, M. Cantoni, M. Veithen, P. Ghosez, K. Johnston, K. M. Rabe, and J. M. Triscone, Phys. Rev. Lett. **95**, 177601 (2005).
[11]J. Y. Jo, R. J. Sichel, H. N. Lee, S. M. Nakhmanson, E. M. Dufresne, and P. G. Evans, Phys. Rev. Lett. **104**, 207601 (2010).
[12]E. Bousquet, M. Dawber, N. Stucki, C. Lichtensteiger, P. Hermet, S. Gariglio, J. M. Triscone, and P. Ghosez, Nature **452**, 732 (2008).
[13]P. Aguado-Puente, P. García-Fernández, and J. Junquera, Phys. Rev. Lett. **107**, 217601 (2011).
[14]H. N. Lee, S. M. Nakhmanson, M. F. Chisholm, H. M. Christen, K. M. Rabe, and D. Vanderbilt, Phys. Rev. Lett. **98**, 217602 (2007).
[15]N. A. Pertsev and B. Dkhil, Appl. Phys. Lett. **93**, 122903 (2008).
[16]N. A. Pertsev, P. E. Janolin, J. M. Kiat, and Y. Uesu, Phys. Rev. B **81**, 144118 (2010).
[17]N. A. Pertsev, A. G. Zembilgotov, and A. K. Tagantsev, Phys. Rev. Lett. **80**, 1988 (1998).
[18]Y. L. Li and L. Q. Chen, Appl. Phys. Lett. **88**, 072905 (2006).
[19]Y. L. Li, L. E. Cross, and L. Q. Chen, J. Appl. Phys. **98**, 064101 (2005).
[20]M. J. Haun, E. Furman, S. J. Jang, H. A. McKinstry, and L. E. Cross, J. Appl. Phys. **62**, 3331 (1987).
[21]$a_{PTO} = 3.935 + 7.312 \times 10^{-5}(T - 298)$,
$a_{BTO} = 3.994 + 5.35386 \times 10^{-5}(T - 273)$,
$a_{STO} = 3.9034 \times (1 + 9.39 \times 10^{-6}(T - 273) + 1.97 \times 10^{-9}(T - 273)^2)$,
where a is the pseudocubic lattice parameter (T in Kelvin), a_{PTO} is redrawn from Ref. 22, a_{BTO} and a_{STO} are obtained from Ref. 23.
[22]P. E. Janolin, F. L. Marrec, J. Chevreu, and B. Dkhil, Appl. Phys. Lett. **90**, 192910 (2007).
[23]Y. L. Li, S. Y. Hu, D. Tenne, A. Soukiassian, D. G. Schlom, X. X. Xi, K. J. Choi, C. B. Eom, A. Saxena, T. Lookman, Q. X. Jia, and L. Q. Chen, Appl. Phys. Lett. **91**, 112914 (2007).
[24]V. R. Cooper and K. M. Rabe, Phys. Rev. B **79**, 180101 (2009).
[25]M. Dawber, N. Stucki, C. Lichtensteiger, S. Gariglio, P. Ghosez, and J. M. Triscone, Adv. Mater. **19**, 4153 (2007).